

Effect of Wind Wave Parameter Fluctuation on the Nonlinear Spectrum Evolution

IGOR V. LAVRENOV

*State Research Center of the Russian Federation, Arctic and Antarctic Research Institute,
St. Petersburg, Russia*

(Manuscript received 29 September 1999, in final form 31 March 2000)

ABSTRACT

The influence of the wind wave parameter fluctuation on the nonlinear spectrum evolution is estimated by solving numerically the kinetic equation taking into account the nonlinear interaction in the wave spectrum. The nonlinear energy transfer is calculated using an original numerical integrating method of the highest accuracy that is described in the paper. The results of numerical simulation shows that wind wave parameter fluctuation produces a significant increase effect of the nonlinear wave spectrum evolution. The present study results in a parameterization, which is made possible taking into account this effect in spectral wind wave models.

1. Introduction

The wind waves are a nonstationary probability process. The evolution of the wind wave field, as is shown by the experimental data, occurs in a wide range of spatial and temporal scales. The period of wave movement fluctuations or simply the period of wave is the shortest temporal scale. The wind wave periods change in a range from several to ten seconds. Their value depends on a number of circumstances (stage of wave development, wind speed, presence of currents, swells, etc.). Their characteristic scale for wind waves in the sea can be considered as a value of $\tau_1 \approx 1\text{--}10$ s.

The wave movements connected with the group wave structure are the second temporal scale (Davidan et al. 1978, 1985). The periods of wave group fluctuations change in a range from several tens to several hundreds of seconds. The wave groups repeat approximately in 10–15 average wave periods ($\tau_2 \approx 10\text{--}15\tau_1$). They consist of five to nine waves. Their temporal recurrence scale, being accepted as the first approximation, makes up $\tau_2 \approx 10^2$ s.

The so-called quasioscillations can be referred to the third temporal fluctuation scale of the sea surface. They are fairly well traced in changes of the frequency spectrum form and in its parameters, even for stable conditions of wave development (Andreev 1988; Zaslavskii and Krasitskii 1993; Bitner-Gregersen and Gran 1983). The quasioscillation periods are approximately equal

from 5 to 20 min. The scale estimation of these periods can be accepted as $\tau_3 \approx 10^3$ s.

Wave field changes, occurring within the period of 3–6 hours, are the fourth temporal scale. This scale is estimated as $\tau_4 \approx 10^4$ s. The essential changes of the wind wave spectrum and all its parameters usually occur within this time interval. It is interesting to note, as far as the temporal scale is concerned, that in numerical simulation of wind wave, with a similar temporal step the data of the surface wind field are input in mathematical models. The mathematical models used for practical application are based on the numerical solution of the wave energy balance equation (Davidan et al. 1985; Komen et al. 1994). The field changes, which occur in smaller temporal and spatial scales, are not taken into account.

The next temporal scale of evolution of the wind wave fields is a synoptic range of order $\tau_5 \approx 10^5$ (Davidan et al. 1978). Numerical simulations of the wind wave in forecasting problems are usually carried out with the help of mathematical models for the intervals of time. The scale variation of the wind wave field (including seasonal, interannual variability, etc.) can be extended, but their detailed consideration is far from the framework of the given article.

It should be noted that all above-mentioned temporal scales of the wind wave field variability differ one from another in order. That is why researchers could investigate the evolution of wave fields in one scale independently from another. But the problem of mutual influence of spatiotemporal evolution of wave field of one scale on another remains to be investigated.

2. Description of the frequency spectrum quasioscillation

Temporal wave records with 20-min duration were obtained in most wind wave field measurements. These

Corresponding author address: Dr. Igor Lavrenov, State Scientific Center of the Russian Federation, Arctic and Antarctic Research Institute, 38 Bering Street, St. Petersburg 199397, Russia.
E-mail: lavren@aari.nw.ru

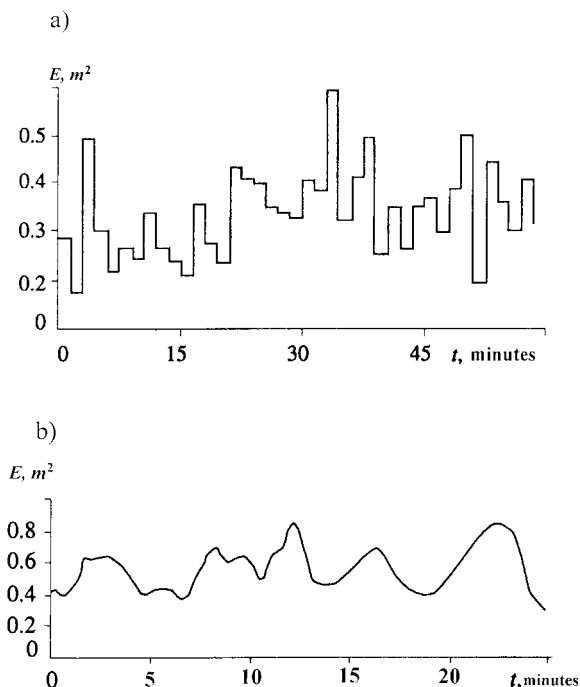


FIG. 1. Proportion $E(t)$ obtained by the running averaging $\eta^2(t)$ (a) for averaging interval 60 s (Zaslavskii and Krasitskii 1993); (b) for averaging interval 150 s (Andreev 1988).

realizations were supposed to be sufficient for obtaining a representative estimation of the wave energy spectral density. This process was considered to be ergodic (Davidan et al. 1978, 1985). The time intervals of such duration were identified as “a quasi-stationary state interval.” It was assumed that the local wave energy defined as $E = \langle \eta^2 \rangle = \int S(\mathbf{k}) d\mathbf{k}$ remains constant, that is, $E = \langle \eta^2 \rangle = \text{const}$ (where $\eta = \eta(\mathbf{r}, t)$ is the sea surface displacement as a function of the spatial coordinate \mathbf{r} and time t and S is the spatial wind wave spectrum). Deviation from this condition was explained as sampling variability of random process.

But this assumption was refuted by research executed in the last decade. The latest data reveal that the condition of constant process dispersion is not valid for a quasistationary interval. Local dispersion makes up a quasiperiodic fluctuation (or simply quasi oscillations) in both the temporal (τ_3) and the corresponding spatial scale range. This phenomenon, well known as smoothed instantaneous wave energy history (SIWEH), was described in Zaslavskii and Krasitskii (1993), Bitner-Gregersen and Gran (1983), Mase (1989), and Sand (1982). The experimental evidence of these existing effects were measurements of local wave dispersion $E = \langle \eta^2 \rangle$ obtained by Zaslavskii and Krasitskii (1993) in the North Atlantic. The experiment was performed under stationary conditions of wave development and in the absence of swell. Obtained for an averaging interval of 60 s, the local dispersion $E(t)$ is shown in Fig. 1a. The fluctuations of wave dispersion $E(t) = \bar{E} + E^1(t)$ with an ~ 5

min temporal scale can be seen. The amplitude $E^1(t)$, comparable with the \bar{E} dispersion, is estimated for a total set. These fluctuations are not dependent upon the group structure of wind waves estimated within a narrow band of their spectrum. The average wave period in this case was 6 s, whereas the temporal scale of wave group was less than 60 s. It is important to note that the estimations of sampling variability were smaller than the fluctuations of wave dispersion, which allows one to observe the phenomenon.

There are data of similar quality in some other papers. An example of time variation of wave dispersion (Andreev 1988) is presented in Fig. 1b. The dispersion was estimated for 150-s intervals with a fluctuation period of 7–15 min. Similar data of variation $E(t)$ with 300-s averaging are obtained in Efimov and Soloviev (1984), where a 15–20 min fluctuation period was estimated.

The local fluctuation of wind wave dispersion is interconnected with fluctuations of the corresponding wave spectra. Such spectral density fluctuations of wave development with 3.5-min long wave records (Andreev 1988) is shown in Fig. 2.

Spectra with limited wave records have the following estimated features:

- measured wave values have various spectral densities and wave dispersions;
- the most conservative parameter is a spectral maximum frequency ω_{\max} , which has approximately the same value during different wave records; and
- the greatest fluctuations in vicinity of the spectral maximum are exhibited in the spectral density.

The sea surface is assumed to respond to low-frequency wind bursts and squalls. This phenomenon can be considered as a quasi oscillation, clearly revealed in changes of frequency spectrum and wave dispersion, even in stable conditions of wave development (Andreev 1988, Zaslavskii and Krasitskii 1993).

It is possible to simulate the aforementioned wave fluctuations of wind wave spectrum parameters by a source function of the wave energy balance equation, which includes the wave energy input by the wind action. The role of gusts in wind wave generation was estimated (Komen et al. 1994) with the WAM model, where the average wind speed was replaced by its random distribution. The effect of gusts was shown to lead to increasing wave energy generation.

There exists a micrometeorological maximum ordering a minute period of the atmospheric turbulence spectra (Monin and Iaglom 1996). Thus the fluctuations of wind wave parameters appear in these temporal scales. A mechanism of wind dispersion generation by atmospheric turbulence can be possibly connected with both pressure and wind speed fluctuations. It should be noted that temporal scales of the micrometeorological maximum in these atmospheric characteristics differ significantly. It is an order of several tens of minutes for the pressure spectra and a minute for wind speed. This qua-

sioscillation period of wave spectral parameters, as shown above, is correlated with the pressure fluctuation of atmospheric turbulence.

It is shown (Zaslavskii and Krasitskii 1993) that the presence of local variant fluctuations within the quasi-stationary state time intervals (τ_3) is a result of spatio-temporal wave field nonuniformity, and it can be described by the kinetic equation for wind wave spectrum evolution. Due to its energy conservation the nonlinear energy transfer was not taken into consideration. The wave dispersion fluctuations were determined by variations of wind-generated waves connected with “micro-meteorological bursts.” Dispersion fluctuations of the sea surface were shown to be quasiperiodical due to changes of the local wave spectrum and, namely, its peakedness.

Due to the existence of general problems of the wind wave theory (Komen et al. 1994; Lavrenov 1998), wave generation by the wind and wave dissipation are not considered here. The effect of wind wave parameter fluctuations on the nonlinear spectrum evolution is studied by introducing a periodically changing term into the energy balance equation. The wave parameter fluctuations produce variations of the spectral form including the peakedness. It causes a local variation of nonlinear energy transfer in the wave spectrum. Taking into account the cubic proportion between the nonlinear energy transfer and the spectrum value, it was interesting to estimate the influence of these variations at the large temporal scales (τ_4/τ_3). The first estimation of this kind was made by Lavrenov (1999), although the value of effect was overestimated. Due to the importance of this problem, we decided to fulfil a more detailed investigation of the quasioscillatory effect, paying attention to the accuracy of nonlinear interaction integral computation.

3. Formulation of the problem

In order to make a quantitative estimation of the physical processes related to quasi oscillations it is necessary to define their parameters. A number of unsolved problems remain, namely the proportion between the oscillation period and spectrum parameters, its peakedness, stage of wave development, etc. Using the results of a previous paper (Zaslavskii and Krasitskii 1993), an elementary approximation of spectral density in the quasi-stationary state interval with quasi oscillations can be presented as an approximation of the JONSWAP spectrum (Hasselmann et al. 1973) with periodic spectral density maximum changes (or spectrum peakedness). This spectrum variation can be presented as

$$S(\omega, \varphi, \omega_{\max}, t) = S_{\text{JONSWAP}}(\omega, \varphi) \gamma^{\mu \sin(2\pi/\tau) f(\omega)}, \quad (1)$$

where $S(\omega, \varphi, \omega_{\max}, t)$ is the frequency–angular spectrum of wind waves; $S_{\text{JONSWAP}}(\omega, \varphi)$ is JONSWAP spectrum with the frequency dependence determined by

$$S_{\text{JONSWAP}}(\omega) = \alpha g^2 \omega^{-5} \exp\left[-\frac{5}{4} \left(\frac{\omega_{\max}}{\omega}\right)^4\right] \gamma^{f(\omega)},$$

$$f(\omega) = \exp\left[-\frac{(\omega - \omega_{\max})^2}{2\sigma\omega_{\max}^2}\right];$$

γ is the spectrum peakedness parameter, μ is the relative oscillation amplitude of the spectral maximum; τ is a period of the oscillations that has a $\tau \sim \tau_3$ order. It should be noted that the temporal dependence of spectral enhancement could be defined in this case as $\tilde{\gamma} = \gamma^{[1 - \mu \sin(2\pi/\tau)]}$.

According to experimental data (Andreev 1988; Zaslavskii and Krasitskii 1993) it is assumed that the frequency of the ω_{\max} spectral maximum changes significantly less at a given time interval than the spectral value as it is. Use of the spectral approximation (1) can be proved by experimental results. The spectral peakedness parameter γ shows a decreasing tendency as waves develop (Mitsuyasu et al. 1980; Donelan et al. 1985; Babanin and Soloviev 1998). The JONSWAP spectrum transforms to the Pierson–Moskowitz spectrum at $\gamma = 1$ in case the fetch X is large enough. High variability of the spectral peakedness parameter γ is well known according to measuring data. It is so high that a systematic dependence $\gamma(\bar{x})$ cannot be found for a wide range of dimensionless fetch changes $\bar{x} = Xg/U^2$. That is why $\gamma(\bar{x})$ dependence was not found in the JONSWAP experiment (Hasselmann et al. 1973).

Now the nonlinear spectrum evolution in the presence of its quasioscillations for a spatially homogeneous case is to be calculated numerically. The following equation is considered:

$$\frac{\partial S}{\partial t} = G_{\text{nl}}(S) - S f_2(\omega) \cos(2\pi t/\tau), \quad (2)$$

where $f_2(\omega) = \mu f(\omega) \ln(\gamma) 2\pi/\tau$; $G_{\text{nl}}(S)$ is the integral of nonlinear interactions in the wind wave spectrum taken relatives to the spectral energy density $S(\omega, \varphi)$.

It is interesting to note that, in case when $G_{\text{nl}}(S)$ is equal to zero, Eq. 2 produces the spectral solution (1). On the other hand, if oscillations are excluded ($f_2(\omega) = 0$), the traditional nonlinear spectral evolution is described by Eq. (2).

Generally the expression for the integral of nonlinear energy transfer relative to the spectral density of wave action $N(k)$ (Hasselmann 1962; Zakharov 1969) is written as

$$G_{\text{nl}}(N) = \iiint T(\mathbf{k}, \mathbf{k}_1, \mathbf{k}_2, \mathbf{k}_3) \delta(\mathbf{k} + \mathbf{k}_1 - \mathbf{k}_2 - \mathbf{k}_3) \delta(\omega + \omega_1 - \omega_2 - \omega_3) \times \{N_2 N_3 (N + N_1) - N_1 N (N_2 + N_3)\} d\mathbf{k}_1 d\mathbf{k}_2 d\mathbf{k}_3, \quad (3)$$

where $N_1 = N(\mathbf{k}_1)$ is the spectral density of wave action, $T(\mathbf{k}, \mathbf{k}_1, \mathbf{k}_2, \mathbf{k}_3)$ is the kernel function of the nonlinear interaction between wave components, and $\delta(\mathbf{k})$ and $\delta(\omega)$ are the Dirac delta functions describing the interaction resonance conditions among four-wave components.

Starting with the fundamental papers (Hasselmann 1962; Zakharov 1968), where the right-hand term of Eq. (2) contains only the nonlinear interaction $G_{nl}(S)$, traditionally it is applied in studying the nonlinear wave spectral evolution. However, isolating the $G_{nl}(S)$ function, the right-hand term of Eq. (2) includes an additional component, periodical in time, that is not used in wind wave models. The second component of the right-hand term of Eq. (2) may be assumed to be an approximation of the mechanism of wave energy supply by the wind and the wave energy dissipation. In reality it is not precisely so. General problems of wave development under wind effect and dissipation are not discussed in this paper. An attempt to describe the spectral evolution due to nonlinear energy transfer and spectral quasioscillation is undertaken below.

In order to solve the problem correctly the quasioscillation period should be large enough for the waves "to have time" to interact, the latter being determined by the characteristic time of phase intermixing (Yuen and Lake 1987):

$$\frac{1}{\tau_{ph}} \approx \omega''(k)(\Delta k)^2, \quad (4)$$

where Δk is the wave spectral width.

The value τ_{ph} appears to be equal to several spectral maximum periods. The condition of applicability of the method can be written as

$$\tau_{ph} \ll \tau_3. \quad (5)$$

It should be noted that in this case the quasioscillation period can be smaller than or of the same order as an evaluation of the characteristic time of nonlinear waves evolution $\tau_{nl} \sim \tau$. The value τ_{nl} can be estimated using Eq. (3) according to Yuen and Lake (1987):

$$\frac{1}{\tau_{nl}} \approx \frac{TN^2}{\omega''(k)(\Delta k)^2}. \quad (6)$$

4. Algorithm and difficulties of numerical calculation of Eq. (2)

The kinetic equation (2) in which the right-hand side term takes into account the presence of a collision integral describing the nonlinear energy transfer and an additional term, which leads the spectral oscillation, is to be solved numerically now. It is necessary to ensure that the temporal step Δt of the numerical integration is much smaller than the oscillation period τ . In this case the numerical solution can take into account the spectral density quasi oscillation. The period τ should be less than the specified time of the nonlinear spectral

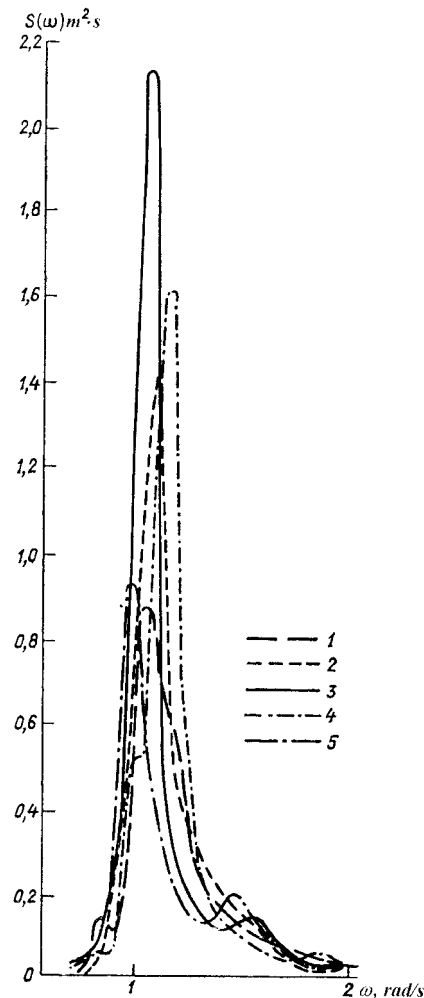


FIG. 2. Spectral density fluctuations of developing waves (1–5) calculated for wave record 3.5-min-long intervals (Andreev 1988).

evolution $\Delta t \ll \tau < \tau_4$. It is necessary to solve numerically Eq. (2) for the large timescale (τ_4/τ_5) using a sufficiently small time step Δt . This is a difficult problem because the numerical computation of nonlinear energy transfer demands considerable CPU time. It means that the algorithm has to be efficient.

The problem of calculating the collision integral of the nonlinear interaction is well known. Although K. Hasselmann deduced the integral of collisions for the first time in the early 1960s, it was really impossible to obtain correct calculation results of the integral in its exact form. To estimate the collision integral numerically is rather a complicated problem. This process needs significant CPU time because, first, the collision integral has the six-dimensional form and, second, the core function $T(\mathbf{k}, \mathbf{k}_1, \mathbf{k}_2, \mathbf{k}_3)$ has a rather complicated form.

In 1980 Masuda (1980) was one of the first to calculate numerically the exact collision integral expression. Using specially selected variables, he estimated

the singularity contribution to the integral value. The calculation process of the integral was in other cases traditional. Then Hasselmann and Hasselmann (1981, 1985a,b) proposed the integral calculation method, based on symmetry of the integral expression, which allowed one to make calculations more quickly.

At present there are three known reliable methods of calculating the collision integral. Resio and Perrie (1991) proposed one of these methods based on the scaling and symmetry of the kernel function. The Snyder et al. (1993) method is based on the hybrid integration scheme for the algorithm of Hasselmann and Hasselmann (1985a,b). It allows one to increase the calculation speed by an order. The third method (RIAM) was proposed by Komatsu and Masuda (1996) as a combination of the Masuda algorithm (1980) with a scaling and symmetry property of the kernel function (Resio and Perrie, 1991). This allows one to increase the calculation speed by two orders.

All of the calculations use traditional methods of numerical integration. Another method, proposed by Lavrenov (1991a, 1998), exists based on the numerical integrating method of the highest precision (Krylov and Shulgina 1966). Using a small number of grid points the collision integral can be quite accurately calculated taking little CPU time. The modified algorithm is presented in the appendix. Calculation of the collision integral (3) is performed using the numerical algorithm. In the present paper Eq. (2) is solved by a two-step predictor–corrector method similar to that of Lavrenov (1991b), allowing one to obtain an accurate numerical solution. The time step of numerical integration was equal to 12.5 s, which made it possible to conduct numerical integration up to a 10^5 s time interval.

5. Results of numerical modeling

In numerical computation the value of parameter μ was assumed to be equal to 0.9, which provided periodic oscillations of spectral enhancement (1) ranging from 1.1 to 9.7 with a mean value $\gamma = 3.3$. The oscillation periods were 10, 20, and 40 min, respectively. The calculation results of the frequency spectra for $\mu = 0.9$ at different moments t (for different values of spectrum peakedness $\tilde{\gamma}$) are presented in Fig. 3a. The spectral density values are normalized by the maximum spectrum value for $\tilde{\gamma} = 3.3$.

The nonlinear transfer function normalized by its maximum value for $\tilde{\gamma} = 3.3$ is presented for the different $\tilde{\gamma}$ in Fig. 3b. Relative values of the nonlinear transfer function differ significantly compared to the corresponding spectral density ones. This is evidence that the proportion between the spectral density and the nonlinear energy transfer function is significantly nonlinear. Changes of spectral influence not only influence significantly the nonlinear energy transfer maximum, but result in changes of nonlinear transfer function in general as well. Magnitudes of the nonlinear energy transfer

and also particular frequencies where the nonlinear energy transfer shows its maximum, minimum, or zero change depend on $\tilde{\gamma}$. For the larger peakedness of the spectrum the nonlinear transfer maximum is shifted to the low-frequency range.

Using the results of spectral numerical solution $S^n(\omega, \varphi)$ at each temporal step t_n , the frequency spectrum maximum S^n_{\max} and the frequency of spectrum maximum ω_{\max} are determined. The computed changes of the frequency spectrum maximum ω_{\max} for four calculation versions are presented in Fig. 4. It is shown for the case of the absence of the spectral maximum oscillations (i.e., $\mu = 0.0$) and for three cases with oscillations of different periods equal to 10, 20, and 40 min, respectively.

A group of data with the same symbols that have the same value of ω_{\max} for different time t means that the frequency ω_{\max} does not change within a considered time interval. At the next time interval the frequency ω_{\max} changes discontinuously. It cannot be explained by the rough frequency discretization used in the numerical scheme. The frequency variation of ω_{\max} is much larger than the frequency discretization step. In total, the evolution of frequency ω_{\max} is not smooth. The discontinuous character of the nonlinear evolution of the spectral maximum frequency shows that the quasi oscillations can be a “start mechanism” of the low-frequency spectrum evolution. It occurs only at a certain moment but not within each quasioscillation period. It takes place in cases when the nonlinear spectral evolution has been accumulated and it changes the spectral form in such a way that it has become enough to make a small push (increasing the spectral density with quasi oscillations) and thus transfer the spectral maximum frequency to another level.

It should be noted that in the “no oscillation” case ω_{\max} does not change for $\gamma = 1$ (i.e., P–M spectrum).

As seen in the calculations, the nonlinear energy transfer produces an average spectral displacement toward the low-frequency range. However, the mean evolution speed of frequency maximum differs significantly when the oscillation spectral peakedness is taken into account. Thus, in the “no oscillation” case the spectral maximum frequency decreases monotonically from the initial value of $\omega_{\max}^0 = 1.88$ rad s^{-1} to $\omega_{\max} = 1.75$ rad s^{-1} for $t = 10^4$ s, to $\omega_{\max} = 1.60$ rad s^{-1} for $t = 3 \times 10^4$ s, and to $\omega_{\max} = 1.47$ rad s^{-1} for $t = 10^5$ s. Oscillations result in a faster decrease of the spectral maximum frequency. The period of oscillation (for the used values) does not significantly effect the general tendency. In the presence of oscillations the spectral maximum frequency decreases from its initial value to $\omega_{\max} = 1.60$ rad s^{-1} for $t = 10^4$ s, to $\omega_{\max} = 1.43$ rad s^{-1} for $t = 3 \times 10^4$ s, and to $\omega_{\max} = 1.30$ rad s^{-1} for $t = 10^5$ s.

As soon as the spectral maximum frequency is the most conservative parameter, comparison of these results show the essential influence of oscillations on the nonlinear spectrum evolution speed. In this case the average speed of spectral maximum displacement is in-

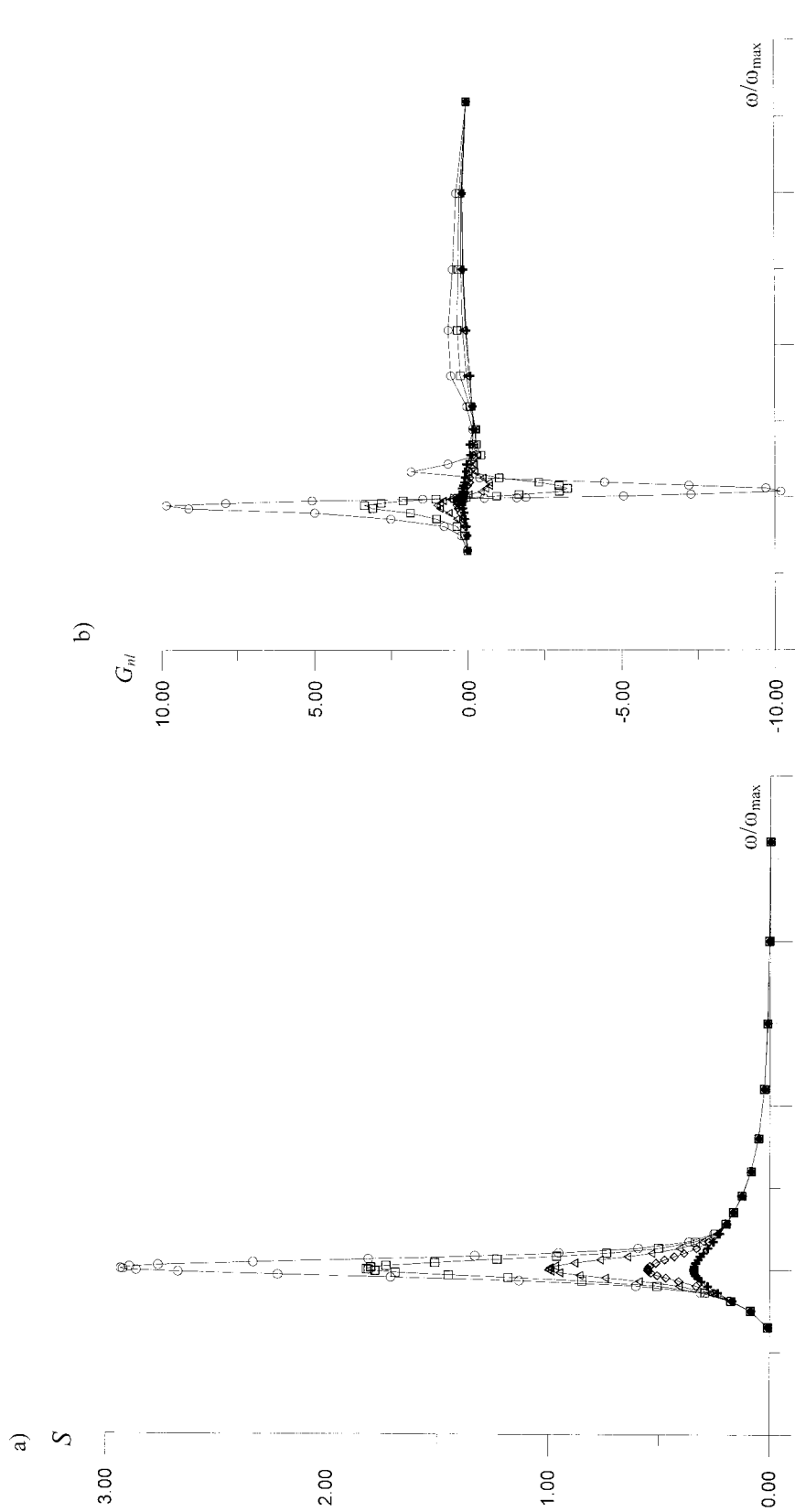


FIG. 3. Numerical calculations results of different quasi-oscillation stages for $\tilde{\gamma} = 1.1$ (+); $\tilde{\gamma} = 1.8$ (\diamond); $\tilde{\gamma} = 3.3$ (Δ); $\tilde{\gamma} = 5.9$ (\square); $\tilde{\gamma} = 9.7$ (\circ); (a) frequency spectra normalized by maximum spectrum value at $\tilde{\gamma} = 3.3$; (b) nonlinear energy transfer functions normalized by its maximum value at $\tilde{\gamma} = 3.3$.

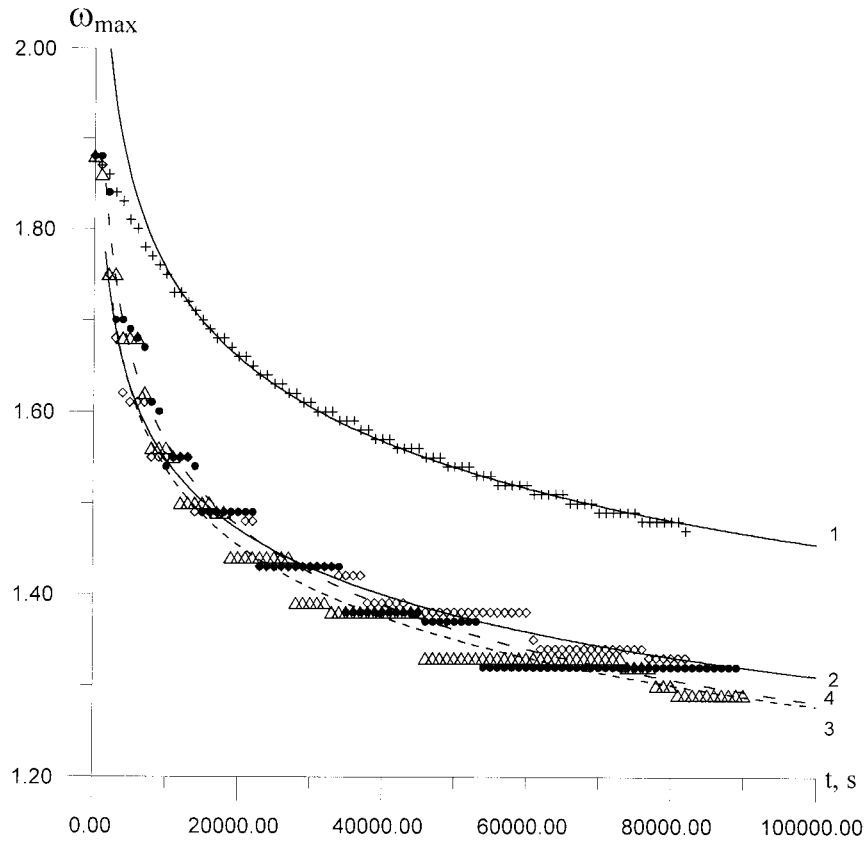


FIG. 4. Frequency evolution of spectrum maximum ω_{\max} determined by nonlinear energy transfer with different period quasi oscillations: 1 (+) without oscillations (approximation $\omega_{\max} \sim 3.73t^{-0.082}$); 2 (\diamond) 10-min oscillation period (approximation $\omega_{\max} \sim 3.01t^{-0.0724}$); 3 (\triangle) 20-min oscillation period (approximation $\omega_{\max} \sim 3.39t^{-0.085}$); and 4 (\bullet) 40-min oscillation period (approximation $\omega_{\max} \sim 3.51t^{-0.0875}$).

creased more than threefold. The numerical simulations show that the average velocity of the spectral maximum displacement depends directly on the quasi-oscillation amplitude of the spectral maximum.

6. Parameterization of the quasio oscillation influence on the nonlinear energy transfer

Wind wave mathematical models produce the approximation of frequency–angular spectrum averaged by a period of the order τ_4 . In this case spectral variations appearing at smaller time periods τ_3 are not taken into consideration. There is a problem of adequate consideration of the quasi-oscillation effect and parameterization of its corresponding contribution to source functions in mathematical models describing the formation of the spectral structure of wind waves.

It is important to point out that fluctuations of the wind wave field, observed in the quasi-stationary state interval, result in significant changes of the spectral form, its peakedness, and wave steepness. That is why local variations of the nonlinear energy transfer appear in the wave spectrum. There is a cubic proportion between the non-

linear transfer and the spectral density. Only a double spectral density increase within its frequency maximum range is able to increase the nonlinear transfer intensity by almost an order of magnitude. The periodic changes of nonlinear energy transfer occur within the quasi-cyclic alterations of its peakedness. When the peakedness within the periods becomes larger in comparison with its average value, the intensity of the nonlinear energy transfer increases. When the peakedness values are small, the nonlinear transfer decreases.

Now an average analytical estimate of the nonlinear energy transfer in the cyclically changed peakedness is to be obtained. According to (3), the first estimation of the nonlinear transfer value is evaluated as $G_{nl}(S) \sim \omega_{\max}^{11} S_{\max}^3 / g^4$. It should be noted that more accurate numerical simulations (see Fig. 3) carried out for the spectrum (1) show that G_{nl} is proportional to S_{\max}^2 rather than to S_{\max}^3 as considered by Lavrenov (1999). Assuming that the maximum frequency ω_{\max} does not change within one cycle and the spectral peak value changes as $S_{\max}(t) \sim \gamma^{\mu \sin(2\pi t/\tau)}$, integration of the nonlinear transfer value within one quasi-oscillation period produces the average as follows:

$$\langle G_{nl} \rangle = \frac{1}{\tau} \int_0^\tau G_{nl}(S(t)) dt = \tilde{G}_{nl} I_0(p), \quad (7)$$

where \tilde{G}_{nl} is a nonlinear transfer without quasi oscillations ($\mu = 0$), I_0 is a modified Bessel function of first order, and the parameter p is determined as $p = 2\mu \ln(\gamma)$. Assuming that $\mu = 1.0$ and $\gamma = 3.3$, it is possible to derive $p \approx 2.39$ (i.e., $p > 1$). The Bessel function (7) is estimated by the following the asymptotic formula (AS USSR 1954):

$$I_0(p) \approx \frac{e^p}{\sqrt{2\pi p}} \left(1 + \frac{1^2}{18p} + \frac{1^2 \cdot 3^2}{2!(8p)^2} + \dots \right). \quad (8)$$

For specific parameter values $I_0 \approx 3.05$ can be obtained. It can be pointed out that the spectral mean over the period for quasi oscillations determined as (1) differs from its corresponding value computed for the “no oscillation” case ($\mu = 0$). The mean spectrum for the same period is equal to

$$\langle S \rangle = \tilde{S} I_0(p/2), \quad (9)$$

where \tilde{S} is the spectral value without quasi oscillations ($\mu = 0$). In (9) the factor is equal to $I_0(p/2) \approx 1.38$. If the nonlinear energy transfer for mean spectrum is recalculated, the value is increased up to a factor of 1.92. It is 1.59 times less than the nonlinear energy transfer with quasi oscillations.

Thus, it can be concluded that the averaged nonlinear energy transfer within the quasi-oscillation period is essentially greater than the value for the average spectrum of the same period of time. An intensive energy flux toward the low-frequency spectral range produces a larger displacement of the spectral maximum frequency toward the low-frequency range.

A simplified approximation of the relative increase of nonlinear energy transfer due to quasi oscillations can be derived from the ratios (8) and (9):

$$\langle G_{nl} \rangle \approx F(p) G_{nl}(\langle S \rangle), \quad (10)$$

where

$$F(p) = \frac{I_0(p)}{I_0(p/2)}, \quad p = 2\mu \ln(\gamma).$$

As a first approximation it is possible to assume that the relative increase of nonlinear energy transfer does not depend on the quasi-oscillation period but is governed by the oscillation amplitude of the spectral maximum μ and the average spectrum peakedness γ . Here F as a function of μ for various values of the parameter γ is presented in Fig. 5. The function F increases monotonically with growing μ and parameter γ . The value of F is equal to 1.0 for $\gamma = 1.0$.

As soon as the peakedness spectral parameter $\gamma \geq 1$ decreases with developing waves (Babanin and Soloviev 1998) the JONSWAP spectrum for unlimited fetch X transforms to the Pierson–Moskowitz spectrum for $\gamma = 1$. The effect of quasi oscillation becomes smaller for

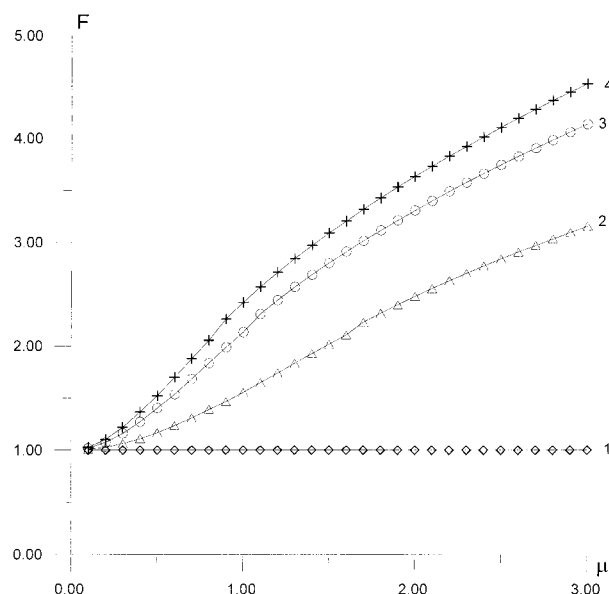


FIG. 5. Proportion between the function F and parameter μ for different values of average spectrum peakedness of γ . 1 (\diamond)— $\gamma = 1.0$; 2 (\triangle)— $\gamma = 3.3$; 3 (\circ)— $\gamma = 7.0$; 4 ($+$)— $\gamma = 10.0$.

the developed wind sea. At the wind wave initial development the quasi oscillation strongly influences the nonlinear evolution.

7. Conclusions

Wind waves are a random, stochastic hydrodynamic process. To simplify the wind wave study a quasi-stationary state interval (on the order of 20 min) was taken (Davidan et al. 1978). The main statistical wave parameters are traditionally considered to remain approximately constant. However, investigations performed during recent decades show that the dispersion and spectrum of the wave process change significantly within this interval. It is important to note that these variations are larger than sample variability.

In the preset study numerical simulations of the energy balance equation are carried out to estimate the influence of the wind wave parameter fluctuation on the nonlinear spectrum evolution. The nonlinear energy transfer within the wave spectrum is calculated using a numerical integrating method of highest accuracy. Results of numerical simulations reveal that the wind wave parameter fluctuation produces a significant increasing effect on the nonlinear wave spectral evolution. Its contribution at the initial stage of wind wave development is most significant. The effect of quasi oscillation becomes smaller for a fully developed wind sea.

The discontinuous character of the nonlinear evolution of the spectral maximum frequency with oscillations (see Fig. 4) shows that quasi oscillations can be a starting mechanism of the low-frequency spectral evolution. However, it does not operate within each quasiooscillation

period, but only at its certain moment. It takes place when the nonlinear spectral evolution has developed enough and changed the spectrum in such a way that it shifts the spectral maximum frequency to another level.

The four-wave energy transfer within the spectrum is a nonlinear mechanism depending on the cube of the spectral density, contrary to the wave energy input by the wind, or quasi-linear wave dissipation (Komen et al. 1994). Therefore the wind wave models usually underestimate the contribution of this mechanism to wave spectral structure development. The nonlinear energy transfer computed for the averaged spectrum is much less than the same total value for the spectrum with quasi oscillations. The present study proposes a parametrization that allows one to take the effect of quasi oscillations into account in the spectral models of wind waves.

Acknowledgments. The paper is supported by the INTAS-1999 (666) project “Estimation of extreme metocean events” and by the Federal Objective Programme-3 “World Ocean” of the Russian Federation.

APPENDIX

Optimal Algorithm of the Nonlinear Energy Transfer Computation

The integral of the nonlinear energy transfer uses the Webb form (1978) of the core function:

$$T(\mathbf{k}, \mathbf{k}_1, \mathbf{k}_2, \mathbf{k}_3) = \frac{\pi g^2 D^2(\mathbf{k}, \mathbf{k}_1, \mathbf{k}_2, \mathbf{k}_3)}{4\rho^2 \omega \omega_1 \omega_2 \omega_3}, \quad (A1)$$

where

$$\begin{aligned} D(\mathbf{k}, \mathbf{k}_1, \mathbf{k}_2, \mathbf{k}_3) = & 2 \left[\frac{(\omega + \omega_1)^2 (k k_1 - \mathbf{k} \mathbf{k}_1) (k_2 k_3 - \mathbf{k}_2 \mathbf{k}_3)}{g |\mathbf{k} + \mathbf{k}_1| - (\omega + \omega_1)^2} + \frac{(\omega - \omega_2)^2 (k k_2 + \mathbf{k} \mathbf{k}_2) (k_1 k_3 + \mathbf{k}_1 \mathbf{k}_3)}{g |\mathbf{k} - \mathbf{k}_2| - (\omega - \omega_2)^2} \right. \\ & \left. + \frac{(\omega - \omega_3)^2 (k k_3 + \mathbf{k} \mathbf{k}_3) (k_1 k_2 + \mathbf{k}_1 \mathbf{k}_2)}{g |\mathbf{k} - \mathbf{k}_3| - (\omega - \omega_3)^2} \right] + \frac{1}{2} [(\mathbf{k} \mathbf{k}_1)(\mathbf{k}_2 \mathbf{k}_3) + (\mathbf{k} \mathbf{k}_2)(\mathbf{k}_1 \mathbf{k}_3) + (\mathbf{k} \mathbf{k}_3)(\mathbf{k}_1 \mathbf{k}_2)] \\ & - \frac{1}{4g^2} [(\mathbf{k} \mathbf{k}_1 + \mathbf{k}_2 \mathbf{k})(\omega + \omega_1)^4 - (\mathbf{k} \mathbf{k}_1 + \mathbf{k}_1 \mathbf{k}_3)(\omega - \omega_2)^4 - (\mathbf{k} \mathbf{k}_3 + \mathbf{k}_1 \mathbf{k}_2)(\omega - \omega_3)^4] \\ & + \frac{1}{g^3} (\omega + \omega_1)^2 (\omega - \omega_2)^2 (\omega - \omega_3)^2 (k + k_1 + k_2 + k_3) + \frac{5}{2} k k_1 k_2 k_3. \end{aligned}$$

Using the symmetry of variables \mathbf{k}_2 and \mathbf{k}_3 the integral (3) can be written as

$$\int d\mathbf{k}_1 \iint d\mathbf{k}_2 d\mathbf{k}_3 = 2 \int d\mathbf{k}_1 \iint_{|\mathbf{k}_2| \leq |\mathbf{k}_3|} d\mathbf{k}_2 d\mathbf{k}_3. \quad (A2)$$

The first integration of (A2) is carried out by \mathbf{k}_3 . Transforming the variables from $\mathbf{k}_i = \{k_{xi}, k_{yi}\}$ to θ_i and to angles $\theta_i = \arctg(k_{yi}/k_{xi})$ and from the wave action $N(\mathbf{k})$ to the wave energy $S(\omega, \theta)$ the expression $N(\mathbf{k}) = (\omega^2/2g^4)S(\omega, \theta)$ is obtained.

The integral (A2) is written in the form

$$G_{nl}(\omega, \theta) = 2 \iiint \iiint T \{ S S_1 (S_2 \omega_3^4 + S_3 \omega_2^4) - S_2 S_3 (S \omega_1^4 + S_1 \omega^4) \} \times \frac{\delta(\omega + \omega_1 - \omega_2 - \omega_3)}{\omega^4 \omega_1^4 \omega_2^4 \omega_3^4} d\omega_2 d\theta_2 d\omega_1 d\theta_1. \quad (A3)$$

Using $\delta(\omega)$ function the (A3) integration by θ_2 gives the following expression:

$$\begin{aligned} G_{nl}(\omega, \theta) = & 4 \sum_{\theta_2} \int_0^\infty \int_{-\pi}^\pi \int_{\omega_2} T \{ S S_1 (S_2 \omega_3^4 + S_3 \omega_2^4) - S_2 S_3 (S \omega_1^4 + S_1 \omega^4) \} \\ & \times \frac{\Theta(\omega_1, \omega_2, \theta_1)}{\omega_1 \omega_2 \omega_3 \sqrt{\omega_a [(k_a + \omega_3^2)^2 - \omega_2^4]} \sqrt{B(\omega_1, \omega_2, \theta_1)}} d\omega_2 d\theta_1 d\omega_1, \quad (A4) \end{aligned}$$

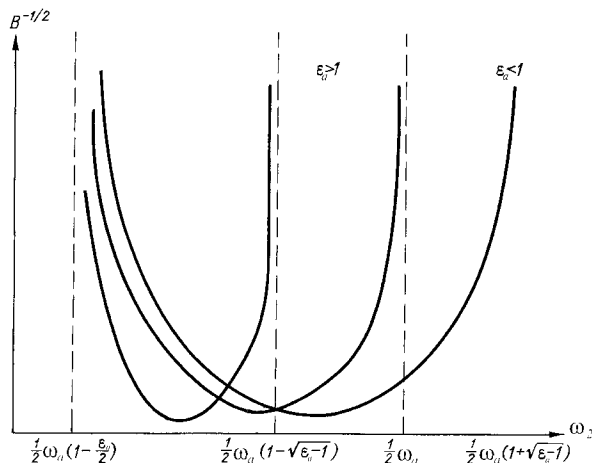


FIG. A1. Function $B^{-1/2}(\omega_2)$ for different value parameter $\epsilon_a = 2k_a/\omega_a^2$.

where

$$\begin{aligned}\omega_a &= \omega_1 + \omega; & \omega_2 &= \omega_a - \omega; \\ k_a^2 &= [\omega_1^4 + \omega^4 + 2\omega^2\omega_1^2 \cos(\theta - \theta_1)];\end{aligned}$$

$$\Theta(\omega_1, \omega_2, \theta_1) = \Theta[2k_a - \omega_a \cos(\theta_2 - \theta_a)]$$

is the Heaviside function:

$$\begin{aligned}\theta_2 &= \theta_a \pm \arccos[(k_a^2 + \omega_2^4 - \omega_a^4)/(2k_a\omega_2^2)]; \\ \theta_3 &= \theta_a \mp \arccos[(k_a^2 + \omega_3^4 - \omega_a^4)/(2k_a\omega_3^2)]; \\ \theta_a &= \arccos[(\omega^2 \cos\theta + \omega_1^2 \cos\theta_1)/k_a] \\ &\quad \times \text{sign}(k_{1y} + k_y).\end{aligned}$$

Function $B = B(\omega_1, \omega_2, \theta_1)$ is written as

$$\begin{aligned}B &= [\omega_2 - \omega_a/2 + k_a/(2\omega_a)] \\ &\quad \times [(\omega_2 - \omega_a/2)^2 - (k_a/2 - \omega_a^2/4)]. \quad (\text{A5})\end{aligned}$$

It should be noted that the function $B = B(\omega_1, \omega_2, \theta_1)$ can be equal to zero at some points (see Fig. A1). It produces the difficulty to integrate (A4) numerically. The most optimal algorithm of integration, which differentiate the present method from others (Hasselmann and Hasselmann 1981; Masuda 1980; Komatsu and Masuda 1996; Polnikov 1989; Resio and Perrie 1991) can be based on utilization of the Jacobi weight functions (Krylov and Shulgina 1966).

In case $\epsilon_a > 1$ (where $\epsilon_a = 2k_a/\omega_a^2$) the integration range is

$$\frac{1}{2}\omega_a(1 - \epsilon_a/2) \leq \omega_2 \leq \frac{1}{2}\omega_a(1 - \sqrt{\epsilon_a - 1}).$$

There are two singularities at the both integration range boundary points (Fig. A1). Using the Jacobi weight functions the integration by σ_2 (in case $\epsilon_a > 1$) can approximated as

$$\begin{aligned}\tilde{F}_1(\omega_1, \theta_1) &= \int_a^b \frac{f_1(\omega_2, \omega_1, \theta_1)}{\sqrt{(\omega_2 - a)(b - \omega_2)}} d\omega_2 \\ &= \frac{\pi}{n} \sum_{j=1}^n f_1(\omega_{2j}, \omega_1, \theta_1), \quad (\text{A6})\end{aligned}$$

where $f_1(\omega_2, \omega_1, \theta_1)$ is a function without singularity;

$$\begin{aligned}a &= \omega_a/2 - k_a/(2\omega_a); & b &= \omega_a(1 - \sqrt{\epsilon_a - 1})/2; \\ \omega_{2j} &= (b + a)/2 + (b - a)/2 \cos[(2j - 1)\pi/2/n].\end{aligned}$$

In case $\epsilon_a < 1$ the range of integration is $\frac{1}{2}\omega_a(1 - \epsilon_a/2) \leq \omega_2 < \frac{1}{2}\omega_a$. At the integration range boundary [i.e., $\omega_2 = \frac{1}{2}(1 - \epsilon_a/2)$] the function $B = B(\omega_1, \omega_2, \theta_1)$ becomes zero (Fig. A1). In this case the following formula can be applied:

$$\begin{aligned}\tilde{F}_2(\omega_1, \theta_1) &= \int_a^d \frac{f_2(\omega_2, \omega_1, \theta_1)}{\sqrt{\omega_2 - a}} d\omega_2 \\ &= \sqrt{d - a} \sum_{j=1}^n A_j f_2(\omega_{2j}, \omega_1, \theta_1), \quad (\text{A7})\end{aligned}$$

where A_j are weight coefficients, ω_{2j} are function ordinates, and $f_2(\omega_2, \omega_1, \theta_1)$ is a function without singularity at the point $\omega_2 = a$. The numerical solution shows (Fig. A2) that it is enough to take $n = 7$ to obtain a good result with a relative error less than 1%–2%. For many practical computation it is enough to use $n = 4$.

The following integration is carried out with respect to θ_1 assuming that the function $\tilde{F}_2(\omega_1, \theta_1)$ is periodical. It is known (Krylov and Shulgina 1966) that the numerical algorithm of the highest precision integration is an ordinary rectangular method:

$$\begin{aligned}\tilde{J}(\omega_1) &= \int_{-\pi}^{\pi} \tilde{F}(\omega_1, \theta_1) d\theta_1 \\ &= \frac{2\pi}{m} \sum_{i=0}^{m-1} \tilde{F}(\omega_1, \theta_{1i} + \xi), \quad (\text{A8})\end{aligned}$$

where $\theta_{1i} = (2\pi/m)i$. In the case where $\xi = \pi/(2m)$ or $\xi = 3\pi/(2m)$, the expression (A8) is valid for $C_m(\theta) = T_{m-1}(\theta) + a_m \cos(m\theta)$, where T_{m-1} is a trigonometrical polynomial with the power of $m - 1$. To get results with error less than 1%–2%, a sufficiently large number of ordinates, that is, $m \geq 90$ is to be taken.

The problem is that the latter integration on θ_1 is not optimal. A large number of ordinates should be used because the function $\tilde{F}(\omega_1, \theta_1)$ includes singularities as well. The function $\tilde{F}(\omega_1, \theta_1)$ becomes infinite in case where $\epsilon_a = 2k_a/\omega_a^2 = 1$. The most effective integration can be achieved by transforming the variables. In this case the Jacobi functions can be used to obtain the cubature formulas. Thus function (A8) can be written

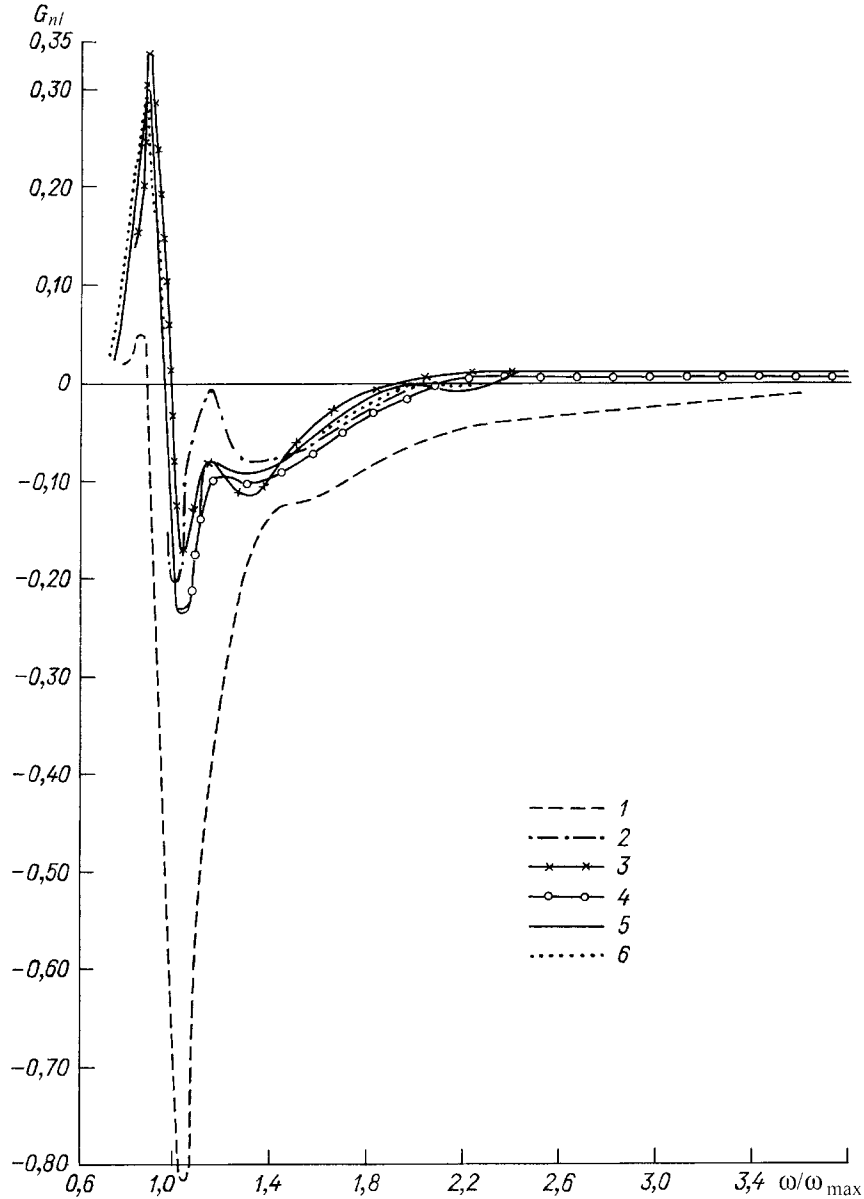


FIG. A2. Calculation of nonlinear energy transfer function using a different number of grid points n in (A5) and (A6): 1) $n = 2$; 2) $n = 3$; 3) $n = 4$; 4) $n = 5$; 5) $n = 7$; 6) $n = 8$.

$$\begin{aligned} \tilde{J}(\omega_1) &= \int_{-\pi}^{\pi} \tilde{F}(\omega_1, \theta_1) d\theta_1 \\ &= \int_{-\pi}^{\pi} \tilde{F}(\omega_1, \theta_1) / \sqrt{|\cos(\theta - \theta_1) - A|} d\theta_1, \quad (\text{A9}) \end{aligned}$$

where

$$\begin{aligned} \tilde{F} &= \tilde{F} \sqrt{|\cos(\theta - \theta_1) - A|}, \\ A &= [(\omega + \omega_1)^4 - 4(\omega_1^4 + \omega^4)] / (8\omega^2\omega_1^2). \end{aligned}$$

The function $A \leq 1$ has its maximum value at the point $\omega = \omega_a$.

Introducing a new variable $x = \cos(\theta - \theta_1)$, the integral (A9) can be presented in the following form:

$$\tilde{J}(\omega_1) = \sum_{\theta_1^{\pm}} \int_{-1}^1 \tilde{F}(\omega_1, \theta_1^{\pm}) \frac{1}{\sqrt{1-x^2}\sqrt{|A-x|}} dx, \quad (\text{A10})$$

where: $\theta_1^{\pm} = \theta \pm \arccos(x)$.

The function $\tilde{F}(\omega_1, x)$ is smooth enough. The integral (A10) includes the same singularities as the first order elliptical integral. Numerical results show that it is enough to use six to eight ordinates to obtain good accuracy.

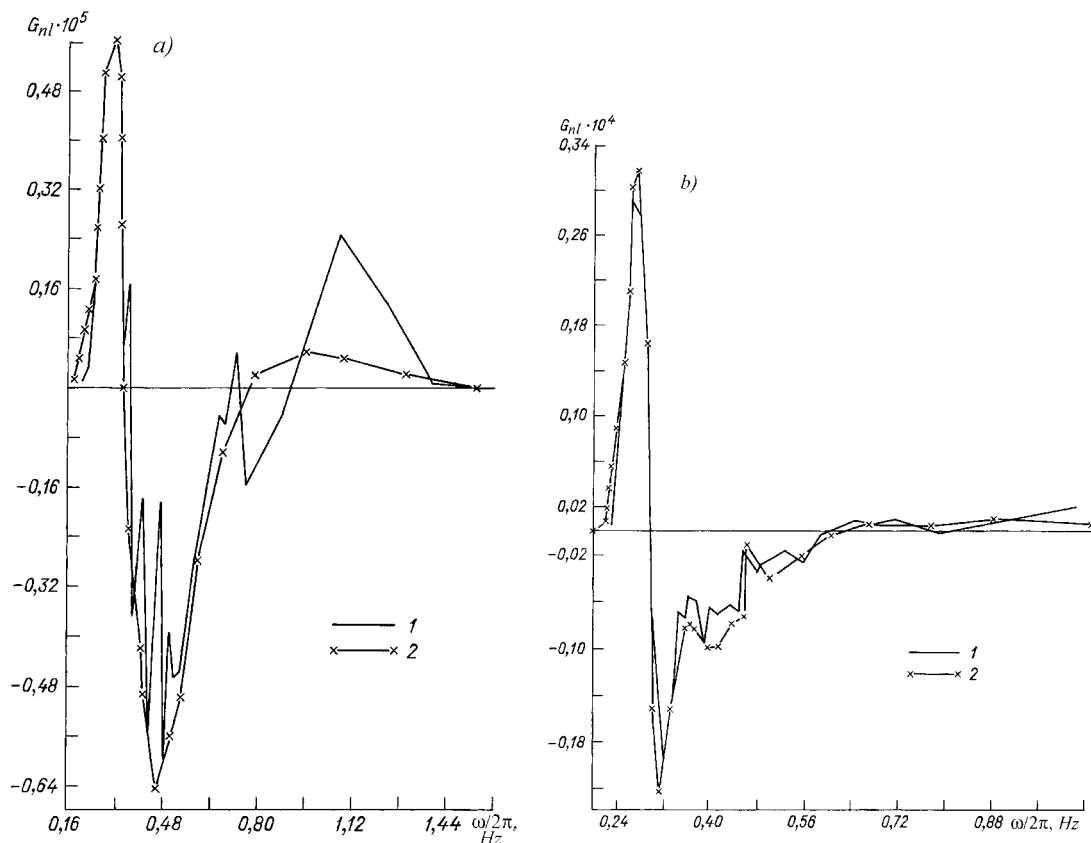


FIG. A3. Numerical results of one-dimensional nonlinear energy transfer function $G_{nl}(\omega)$ for JONSWAP spectrum for two different value of spectrum peakedness $\gamma = 1$ (a) and 3.3 (b), correspondingly. 1) According to paper (K. Hasselmann and S. Hasselmann, 1981); 2) by present algorithm.

The last integration by ω_1 can be carried out effectively taking into account that the function $\tilde{J}(\omega_1)$ is approximated as $\tilde{J}(\omega_1) \sim \omega_1^{-6}$ for a large values of ω_1 , and as $\tilde{J}(\omega_1) \sim \omega_1^{5+25}$ for small values ω_1 . It allows one to use the traditional cubature method of integration. It also allows one to use the traditional cubature method of integrating (Lavrenov, 1998). It should be noted that to speed up the procedure of computation, the part of function in (A4) that does not depend on the spectral value is computed using the symmetry quantity (Hasselmann and Hasselmann 1981).

As an example Figs. A3a and A3b present the numerical results of one-dimensional nonlinear energy transfer $G_{nl}(\omega)$ for JONSWAP spectrum for two different value of spectrum peakedness: $\gamma = 1$ and 3.3, correspondingly. For comparison the results of Hasselmann and Hasselmann (1981) are presented as well to show the stability of our algorithm.

It should be noted that the main advantage of the algorithm is that integration is based on a relatively smaller number of grid points compared to the usual methods. It speeds up the computation at least by two orders (Lavrenov 1998).

REFERENCES

- Andreev, B. M., 1988: Variability of spectral characteristics of wave developing. *Theoretical Foundations and Calculation Methods of Wind Waves* (in Russian), Gidrometeoizdat, 75–81.
- AS USSR, 1954: Tables with Bessel function means of an imaginary argument (in Russian). AS USSR, 1–258.
- Babanin, A. V., and Y. P. Soloviev, 1998: Field investigation of transformation of the wind wave frequency spectrum with fetch and stage of development. *J. Phys. Oceanogr.*, **28**, 563–576.
- Bitner-Gregersen, E., and S. Gran, 1983: Local properties of sea waves derived from a wave record. *Appl. Ocean Res.*, **5**, 210–214.
- Davidan, I. N., L. I. Lopatukhin, and V. A. Rozhkov, 1978: *Wind Waves as Probability Hydrodynamic Process* (in Russian). Gidrometeoizdat, 285 pp.
- , and Coauthors, 1985: *Wind Waves in the World Ocean* (in Russian). Gidrometeoizdat, 256 pp.
- Donelan, M. S., and Coauthors, 1985: Directional spectra of wind-generated waves. *Philos. Trans. Roy. Soc. London*, **A315**, 509–562.
- Efimov, V. V., and Y. P. Soloviev, 1984: Low frequency sea level oscillations and wind waves group structure. *Izv. Acad. Sci. USSR. Atmos. Oceanic Phys.*, **20**, 985–994.
- Hasselmann, K., 1962: On the non-linear energy transfer in a gravity wave spectrum. Part I. *J. Fluid Mech.*, **12**, 481–500.
- , 1963: On the non-linear energy transfer in a gravity wave spectrum. Part 2. *J. Fluid Mech.*, **15**, 273–281.
- , and Coauthors, 1973: Measurements of wind-waves growth

- and swell decay during the Joint North Sea Wave Project (JONSWAP). *Deutsch. Hydrogr. Inst.*, 95 pp.
- Hasselmann, S., and K. Hasselmann, 1981: A symmetrical method of computing the nonlinear transfer in a gravity wave spectrum. *J. Hamburger Geophys. Einzelschriften*, **52**, 138 pp.
- , and —, 1985a: Computations and parametrizations of the non-linear energy transfer in gravity-wave spectrum. Part I: A new method of the nonlinear energy transfer integral. *J. Phys. Oceanogr.*, **15**, 1369–1377.
- , and —, 1985b: The model EXACT-NL. *Ocean Wave Modelling (The SWAMP Group)*, Plenum Press, 249–251.
- Komatsu, K., and A. Masuda, 1996: A new scheme of nonlinear energy transfer among wind waves: RIAM method. Algorithm and performance. *J. Oceanogr.*, **52**, 509–537.
- Komen, G. J., L. Cavaleri, M. Donelan, K. Hasselmann, S. Hasselmann, and P. A. E. M. Janssen 1994: *Dynamics and Modelling of Ocean Waves*. Cambridge University Press, 532 pp.
- Krylov, V. I., and E. T. Shulgina, 1966: *Manual on a Numerical Integration* (in Russian). Nauka, 371 pp.
- Lavrenov, I. V., 1991a: Non-linear interaction in rips spectrum. *Izv. Acad. Sci. USSR. Atmos. Oceanic Phys.*, **27**, 438–447.
- , 1991b: Non-linear evolution of wave spectrum in shallow water area. *Izv. Acad. Sci. USSR. Atmos. Oceanic Phys.*, **27**, 1373–1378.
- , 1998: *Mathematical Modelling of Wind Waves at Non-Uniform Ocean* (in Russian). Gidrometeoizdat, 500 pp.
- , 1999: The effect of quasi-oscillations in wind wave spectrum on its low-frequency non-linear evolution. *Izv. Acad. Sci. USSR. Atmos. Oceanic Phys.*, **35**, 339–405.
- Mase, H., 1989: Goupiness factor and wave height distribution. *J. Wat., Port, Coast Ocean Eng.*, **115**, 105–121.
- Masuda, A., 1980: Nonlinear energy transfer between wind waves. *J. Phys. Oceanogr.*, **10**, 2082–2093.
- Mitsuyasu, H., F. Tasai, T. Suhara, S. Mizuno, M. Ohkusu, T. Honda, and K. Rikiihi, 1980: Observation of the power spectrum of ocean waves using a clover leaf buoy. *J. Phys. Oceanogr.*, **10**, 286–296.
- Monin, A. S., and A. M. Iaglom, 1996: *Statistical Hydrodynamics*. Part 2. Gidrometeoizdat, 742 pp.
- Polnikov, V. G., 1989: Calculation of non-linear energy transfer by surface gravitational waves spectrum. *Izv. Acad. Sci. USSR. Atmos. Oceanic Phys.*, **25**, 1214–1225.
- Resio, D., and W. Perrie, 1991: A numerical study of nonlinear energy flux due to wave-wave interaction. Part 1. Methodology and basic results. *J. Fluid Mech.*, **223**, 603–629.
- Sand, S., 1982: Wave grouping described by bundled long waves. *Ocean Eng.*, **9**, 567–579.
- Snyder, R. L., W. C. Thacker, K. Hasselmann, S. Hasselmann, and G. Barzel, 1993: Implementation of an efficient scheme for calculating nonlinear transfer from wave-wave interaction. *J. Geophys. Res.*, **98**, 14 507–14 524.
- Webb, D. J., 1978: Non-linear transfer between sea waves. *Deep-Sea Res.*, **25**, 279–298.
- Yuen, G., and A. Lake, 1987: *Nonlinear Dynamics of Gravitational Waves in Deep Water*. Mir, 180 pp.
- Zakharov, V. Ye., 1968: Stability of periodic waves of final amplitude on a deep liquid surface. *PMTF*, **2**, 86–94.
- Zaslavskii, M. M., and V. P. Krasitskii, 1993: About wave fluctuations of wind waves spectrum parameters. *J. Okeanologia*, **33**, 21–26.